arXiv:1606.00084v1 [astro-ph.SR] 1 Jun 2016

Study of young stellar objects around SNR G18.8+0.3

M. Celis Peña[1] and S. Paron[1]

[1]Instituto de Astronomía y Física del Espacio (IAFE)

2 de junio de 2016

Abstract

In recent works, through observations of molecular lines, we found that the supernova remnant (SNR) G18.8+0.3 is interacting with a molecular cloud towards its southern edge. Also it has been proven the presence of several neighboring HII regions very likely located at the same distance as the remnant. The presence of dense molecular gas and the existence of shock fronts generated by the SNR and HII regions make this region an interesting scenario to study the population of young stellar objects. Thus, using the most modern colour criteria applied to the emission in the mid-infrared bands obtained from IRAC and MIPS on board Spitzer, we characterized all the point sources lying in this region. We analyzed the spectral energy distributions of sources that show signs of being young stellar objects in order to confirm their nature and derive stellar parameters. Additionally, we present a map of the ^{12}CO J=3-2 emission obtained with the ASTE telescope towards one of the HII regions embedded in the molecular cloud. The molecular gas was studied with the aim to analyze whether the cloud is a potential site of star formation.

Resumen

Recientemente, a través de observaciones de líneas moleculares hemos comprobado que el remanente de supernova (RSN) G18.8+0.3 se encuentra interactuando con una nube molecular hacia su borde sur. También se ha comprobado la presencia de varias regiones HII vecinas asociadas al gas molecular, las cuales muy probablemente se encuentran a la misma distancia que el remanente. La presencia de gas molecular denso, y la existencia de frentes de choque, generados tanto por el RSN como por las regiones HII, convierten a esta región en un interesante escenario en donde estudiar la población de objetos estelares jóvenes. De esta manera, utilizando los criterios de color más modernos aplicados a la emisión de las bandas del infrarrojo medio obtenidas de los instrumentos IRAC y MIPS a bordo del satélite Spitzer, se caracterizaron todas las fuentes puntuales

que yacen en esta región. A aquellas que presentan indicios de ser objetos estelares jóvenes se les analizó su distribución espectral de energía, con el fin de confirmar su naturaleza y extraer varios parámetros estelares. De manera adicional se presenta un mapa de la emisión del ^{12}CO J=3-2 obtenido con el telescopio ASTE hacia una de las regiones HII vecinas al RSN. Se realizó una caracterización del gas molecular con el fin de analizar si la nube es un potencial sitio de formación estelar activa.

1. Introduction

The interaction between the supernova remnant (SNR) G18.8+0.3 and a molecular cloud was analyzed in recent works. The molecular gas belonging to regions 1 and 2 (see Figure 1) was studied in Paron et al. [2012] and Paron et al. [2015], respectively. The presence of abundant molecular gas, several embedded HII regions and the SNR, makes this region an interesting scenario to study possible triggered star formation. Thus, in this work we present a study of the distribution of the young stellar objects (YSOs) in the SNR surroundings. In addition, we study the molecular gas towards the named region 3 in Figure 1, which is related to the HII region G018.584+00.344.

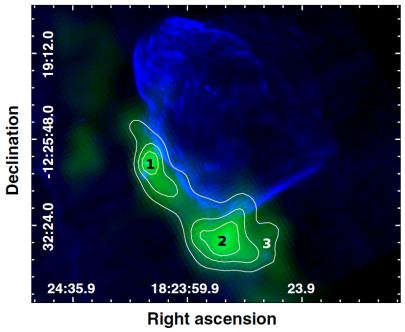

Figure 1: SNR G18.8+0.3 in radio continuum emission at 20 cm (blue) and the integrated ^{13}CO J=1–0 emission extracted from the Galactic Ring Survey (green).

2. Results

2.1. Young stellar objects

We search for YSO candidates towards a region of about 5′ in size around the SNR G18.8+0.3. Using the GLIMPSE Point-Source Catalog acquired by Spitzer-IRAC (at 3.6, 4.5, 5.8 and 8 μm) we selected sources following the criteria presented in Gutermuth et al. [2009]. We found 9 Class I objects and 47 Class II objects, white and magenta crosses in Figure 2, respectively, which are displayed over a three-colour image with the radio continuum emission at

Table 1: Stellar parameters obtained from the SEDs.

Source	$M_\star$ $[M_\odot]$	Range $M_\star$	Age $[10^5 \mathrm{yr}]$	Range Age	$\dot{M}_{\mathrm{env}}$ $[10^{-3} M_\odot \mathrm{yr}^{-1}]$	Range $\dot{M}_{\mathrm{env}}$	L $[10^3 L_\odot]$	Range L	χ^2_{best}	Satisfying models	Stage
1	16.3	–	12.5	–	0	–	26.7	–	52.4	10	III
2	10.0	5.7–15.2	15.5	11.4–47.0	0	–	6.2	1.2–21.6	1.0	305	II
3	9.1	5.9–13.6	0.01	0.01–37.7	1.4	0–6.6	0.2	0.9–11.8	3.2	23	0-I
4	7.8	1.0–11.5	31.4	0.01–67.6	0	0–0.5	2.5	0.2–9.8	0.7	706	II
5	18.8	17.8–19.9	12.8	12.8–14.5	0	–	39.6	34.1–46.2	63.2	15	III
6	18.5	16.4–20.9	13.1	13.0–14.3	0	–	37.9	26.9–50.1	69.3	27	III
7	8.0	–	0.4	–	0.5	–	0.9	–	15.1	2	0-I
8	13.9	6.7–16.3	15.5	0.02–24.6	0	0–0.6	17.1	0.9–26.7	3.7	203	II
9	4.3	3.2–6.9	20.5	0.8–78.1	0	0–0.9	0.2	0.1–1.6	0.1	461	II
10	7.0	7.0–9.8	18.5	10.9–43.8	0	–	2.0	1.9–5.9	10.2	98	II
11	14.4	8.7–23.8	0.06	0.01–24.6	1.2	0–4.4	7.6	4.0–30.7	1.3	71	0-I
12	8.1	7.2–10.8	21.7	0.6–32.1	0	0–1.8	3.0	2.1–8.0	12.4	32	II
13	16.3	–	12.5	–	0	–	26.7	–	77.4	10	III
14	18.5	18.5–20.6	13.1	13.0–13.1	0	–	37.9	37.9–50.1	26.0	16	III
15	15.6	9.9–19.9	16.3	11.8–32.6	0	–	23.4	6.2–45.9	47.1	33	III
16	16.3	–	12.5	–	0	–	26.7	–	148.7	9	II
17	13.9	13.9–19.9	18.2	13.8–18.2	0	–	19.0	19.0–46.2	39.7	14	II
18	15.6	13.6–19.9	16.3	11.8–16.3	0	–	23.4	15.8–45.9	39.2	19	III
19	16.9	15.7–18.8	12.4	12.4–19.3	0	–	29.3	23.7–39.6	74.6	34	II
20	4.8	4.4–7.2	9.5	0.6–60.3	10^{-4}	0–0.6	0.4	0.1–1.6	0.0	340	II
21	3.9	3.1–5.7	52.1	3.6–92.6	0	0–0.05	0.1	0.1–0.7	0.7	205	II
22	11.5	7.2–13.7	19.5	11.6–38.4	0	–	9.8	2.5–16.3	4.3	58	II
23	18.5	–	13.1	–	0	–	37.9	–	34.3	10	III
24	9.6	9.4–15.8	30.3	18.7–30.3	0	–	5.5	5.1–24.4	36.2	25	III
25	6.2	4.6–7.9	31.1	10.9–59.8	0	–	1.0	0.4–2.7	1.73	219	II
26	9.7	7.4–10.8	17.8	13.6–32.6	0	–	5.7	2.1–8.1	83.3	52	III
27	16.9	12.0–17.9	12.4	12.4–22.2	0	–	29.3	11.5–34.4	53.6	32	II
28	16.4	16.3–18.6	14.3	12.5–14.3	0	–	26.9	26.7–38.3	60.6	28	III
29	12.0	11.9–12.0	22.2	15.3–22.2	0	–	11.5	11.3–12.1	74.2	6	II
30	9.9	9.9–15.6	32.6	13.8–32.6	0	–	6.2	6.2–23.4	42.7	27	III

A "–" in the range columns means that all the satisfaying models share the same value as the best-fit model.

20 cm presented in blue, the submillimeter continuum emission at 870 μm in green, and the 8 μm emission in red. It can be appreciated that some YSO candidates are related to cold dust condensations mapped by the submillimeter continuum. Thirty of these objects have their fluxes measured at 24 μm with MIPS-Spitzer, and thus for these sources we performed an analysis of its spectral energy distribution (SED) using the tool developed by Robitaille et al. [2007] and available online [1]

To build the SEDs models we used the Spitzer-IRAC fluxes measured in the bands 3.6, 4.5, 5.8, 8.0 μm and the flux at 24 μm measured with Spitzer-MIPS. Using the criteria presented in Robitaille et al. [2006], the YSO candidates can be classified in:

> Stage 0-I: objects with significant infalling envelopes and possibly disks. This stage is defined by $\dot{M}_{env}/M_\star > 10^{-6} yr^{-1}$, where $\dot{M}_{env}$ is the envelope accretion rate, and $M_\star$ is the central source mass.
>
> Stage II: objects with optically thick disks (and possible remains of a tenuous infalling envelope). This stage is defined by $\dot{M}_{env}/M_\star < 10^{-6} yr^{-1}$ and $M_{disk}/M_\star > 10^{-6} yr^{-1}$, where M_{disk} is the disk mass.
>
> Stage III: objects with optically thin disks. This stage is defined by $\dot{M}_{env}/M_\star < 10^{-6} yr^{-1}$ and $M_{disk}/M_\star < 10^{-6} yr^{-1}$.

Table 1 presents some stellar parameters obtained from the SED of each source. The parameters from the best fit model and their ranges obtained from

[1] http://caravan.astro.wisc.edu/protostars/

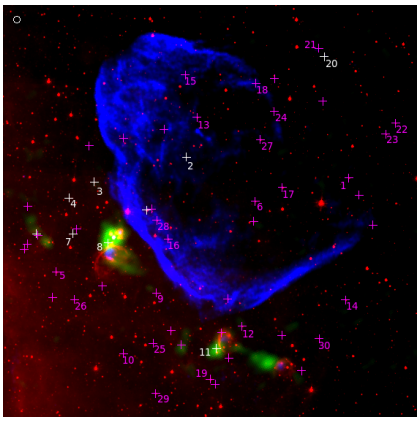

Figure 2: SNR G18.8+0.3 in radio continuum emission at 20 cm (blue), submillimeter continuum at 870 μm from ATLASGAL (green), and 8 μm emission from IRAC-Spitzer (red). White and magenta crosses are Class I and II sources according Gutermuth et al. [2009].

all the satisfying models are presented. To do this, we selected the models that satisfied the condition $\chi^2 - \chi^2_{\rm best} < 3N$, where $\chi^2_{\rm best}$ is the minimum value of the χ^2 among all models, and N is the number of input data fluxes. Additionally the source stage is included in the last column of the table.

Taking into account our photometric and SED analysis of the sources and their spacial distribution towards the SNR and the associated molecular cloud, we conclude that there is no evidence that allow us to infer triggered star formation in the region. Additionally, performing a SED to the embedded HII regions (see Paron et al. [2012, 2015]), it is concluded that they are located at the same distance as the SNR (about 8 kpc). With this in mind, and assuming that many of the sources analyzed here are at the same distance, we conclude that we are studying a region populated by many massive stars in different evolutive stages.

2.2. Molecular gas analysis towards the HII region G018.584+00.344

Using molecular data obtained with the Atacama Submillimeter Telescope Experiment (ASTE) (see Paron et al. [2015] for a description of the observations), we investigated the interstellar medium around the HII region G018.584+00.344 which lies southwards the SNR G18.8+0.3 (region 3 in Fig.1). Figure 3 is a three-colour image where the radio continuum emission at 20 cm is presented in blue, the 8 μm emission in red, and the integrated ^{12}CO J=3–2 emission obtained with ASTE in green. The molecular peak, located estwards the HII region G018.584+00.344, coincides with an ATLASGAL submillimeter continuum source, showing an excellent correlation between the molecular gas and cold dust.

From the molecular feature defined by the 50 K km s^{-1} contour in Fig.3 we estimated the molecular mass from three independent ways: using the measured

CO luminosity, from the cold dust emission, and through tha virial theorem. The results are:

$$M_{\rm COlum} \sim 8.5 \times 10^3 M_\odot$$
$$M_{\rm dust} \sim 5.7 \times 10^3 M_\odot$$
$$M_{\rm vir} \sim 8.2 \times 10^3 M_\odot$$

From the comparison between the obtained mass values, it is concluded that the molecular clump is gravitationally bound, and taking into account that there is not any YSO candidate embedded in it, we suggest that it is a quiescent molecular clump.

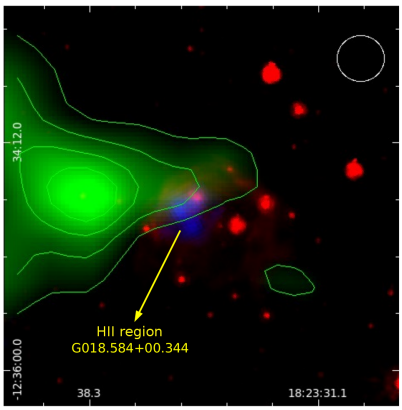

Figure 3: Radio continuum emission at 20 cm (blue), IR emission at 8 μm (red), and the ^{12}CO J=3–2 integrated between 15 and 30 km s^{-1} emission (green), with contours levels of 30, 40, 50 and 60 K km s^{-1}. The beam of the molecular observations is presented at the top right corner.

3. Acknowledgement

S.P is member of the *Carrera del investigador científico* of CONICET, Argentina. M.C.P is a doctoral fellow of CONICET, Argentina. This work was partially supported by Argentina grants awarded by UBA (UBACyT), CONICET and ANPCYT.

References

RA Gutermuth, ST Megeath, PC Myers, LE Allen, JL Pipher, and GG Fazio. A spitzer survey of young stellar clusters within one kiloparsec of the sun: cluster core extraction and basic structural analysis. *The Astrophysical Journal Supplement Series*, 184(1):18, 2009.

S Paron, ME Ortega, A Petriella, M Rubio, G Dubner, and E Giacani. The molecular clump towards the eastern border of snr g18. 8+ 0.3. *Astronomy & Astrophysics*, 547:A60, 2012.

S Paron, M Celis Peña, ME Ortega, A Petriella, M Rubio, G Dubner, and E Giacani. The southern molecular environment of snr g18. 8+ 0.3. *Astronomy & Astrophysics*, 580:A51, 2015.

Thomas P Robitaille, Barbara A Whitney, Remy Indebetouw, Kenneth Wood, and Pia Denzmore. Interpreting spectral energy distributions from young stellar objects. i. a grid of 200,000 yso model seds. *The Astrophysical Journal Supplement Series*, 167 (2):256, 2006.

Thomas P Robitaille, Barbara A Whitney, Remy Indebetouw, and Kenneth Wood. Interpreting spectral energy distributions from young stellar objects. ii. fitting observed seds using a large grid of precomputed models. *The Astrophysical Journal Supplement Series*, 169(2):328, 2007.